UNLIMITED

Tech Memo
P 1198

Tech Memo
P 1198

ROYAL AEROSPACE ESTABLISHMENT

Technical Memorandum

December 1990

Unsteady Viscous Flow in a High Speed Core Compressor

by

M. A. Cherrett
J. D. Bryce

Procurement Executive, Ministry of Defence
Farnborough, Hampshire

CONDITIONS OF RELEASE

0093679 BR-116642

MR PAUL A ROBEY
DTIC
Attn DTIC-FDAC
Cameron Station-Bldg 5
Alexandria
VA 22304 6145
USA

********** DRIC U

********** DRIC Y

Reports quoted are not necessarily available to members of the public or to commercial organisations.

LIST OF CONTENTS

ROYAL AEROSPACE ESTABLISHMENT

Technical Memorandum P 1198

Received for printing 10 December 1990

UNSTEADY VISCOUS FLOW IN A HIGH SPEED CORE COMPRESSOR

by

M. A. Cherrett

J. D. Bryce

SUMMARY

A probe incorporating a miniature high-frequency response pressure transducer has been traversed behind the first three stages of a high-speed multistage compressor operating at throttle settings corresponding to near choke, peak efficiency and near surge. A novel method of compensating for transducer temperature sensitivity was employed. Consequently, time-averaged pressures derived from the transducer were found to be in good agreement with pneumatic pressure measurements. Analysis of the unsteady pressure measurements revealed both the periodic and random fluctuations in the flowfield. This provided information on rotor-rotor interaction effects and the nature of viscous blade wake and secondary flows in each stage.

This Memorandum is a facsimile of a paper prepared for the 36th ASME International Gas Turbine and Aerengine Congress and Exposition to be held in Orlando, Florida, USA, 3-6 June 1991.

UNLIMITED

UNSTEADY VISCOUS FLOW IN A HIGH SPEED CORE COMPRESSOR

M A Cherrett and J D Bryce
Propulsion Department
Royal Aerospace Establishment
Pyestock
Farnborough
Hants UK

ABSTRACT

A probe incorporating a miniature high-frequency response pressure transducer has been traversed behind the first three stages of a high-speed multistage compressor operating at throttle settings corresponding to near choke, peak efficiency and near surge A novel method of compensating for transducer temperature sensitivity was employed Consequently, time-averaged pressures derived from the transducer were found to be in good agreement with pneumatic pressure measurements Analysis of the unsteady pressure measurements revealed both the periodic and random fluctuations in the flowfield This provided information on rotor-rotor interaction effects and the nature of viscous blade wake and secondary flows in each stage

INTRODUCTION

Further improvements in the efficiency, stage-loading, and stable operating range of compressors rely heavily upon developing improved computational flow modelling and design methods In turn, the improvement of computational methods requires detailed measurements to be taken in representative compressors to create data bases for code validation A number of workers have undertaken detailed measurements of the flow in axial compressors Ravindranath & Lakshminarayana (1980) and Lakshminarayana & Govindan (1981) investigated the characteristics of blade wake development while Dring et al (1983), Lakshminarayana et al (1985) and Dong et al (1987) extended these studies to include secondary flow development in the hub and tip regions Further, Wagner et al (1978) and Zeirke & Okiishi (1982) investigated the effects of bladerow interaction These studies have done much to improve understanding of axial compressor flows and highlighted the complex, viscous, three-dimensional, interactive, and unsteady nature of the flowfield However, all the cited studies have been limited to low-speed research compressors Therefore, although blade geometry and stage loading may be representative of aero-engine compressors, flow Mach numbers are not Published measurements taken in high-speed compressors have been limitea to single stage transonic fans (Weyer & Hungenberg (1976), Ng & Epstein (1985) and Gertz (1986) These indicate significant flowfield unsteadiness that has been attributed to shock oscillation While the mechanism producing these unsteady effects has yet to be explained fully, it is likely that their existence, along with quasi-steady compressibility effects, have a significant influence upon the development of wake and endwall flows. Matters are further complicated by complex interaction between the stages within multistage compressors Hence it is necessary to carry out investigations within high-speed (engine-relevant) compressors in order to improve the fundamental understanding of the phenomena involved and to explore the applicability of low-speed data for computational code validation

Propulsion Department of the Royal Aerospace Establishment (RAE) is engaged in a programme to employ high frequency response instrumentation to investigate unsteady viscous flow within high-speed axial compressors and fans The work reported in this paper documents preliminary activity 'piggy-backed' onto a major conventional rig measurement programme reported by Ginder (1991) A single sensor probe, containing a high-frequency response pressure transducer, was used to measure the unsteady flow within the first three stages of the five-stage C147 high-speed core compressor Errors due to temperature sensitivity of the pressure transducer were corrected using a combination of careful calibration and an expedient method of measuring transducer diaphragm temperature This system is described, together with the data acquisition and processing techniques employed The time-averaged pressures derived from the compensated transducer signals are compared with conventional pneumatic measurements to illustrate the success of the method. Finally, unsteady pressure measurements taken at rotor exit are presented and discussed

EXPERIMENTAL PROCEDURE

The Test Compressor

The RAE C147 research compressor is a high-speed machine representative of the rearmost stages of a military or highly loaded civil core compression system. It is of large scale, approximately 1 m in diameter, with extended axial gaps between the blade rows to allow detailed traverse measurements to be taken To date it has been tested in two configurations. The initial build, reported by Calvert et al (1989), was a four stage compressor of 4.0 pressure ratio For the second build, the blading was redesigned using the RAE S1-S2 calculation system (also described by Calvert et al

TM P 1198

(1989)) and a zero stage added. Because the second build evolved from a 4-stage predecessor the convention of referring to stages as stage 0 through to stage 4 is adopted throughout the paper. This five stage machine was designed to deliver a pressure ratio of 6.4 at a flowrate of 49.5 kg/s and is referred to by Ginder (1991)

Unsteady pressure measurements were taken in the second build of C147. Radial traverses were carried out behind rotors 0, 1 and 2 while the compressor was operating at three conditions on the 95% speed characteristic. The operating points, defined as near choke (A), peak efficiency (B) and near surge (C), are shown in Fig 1.

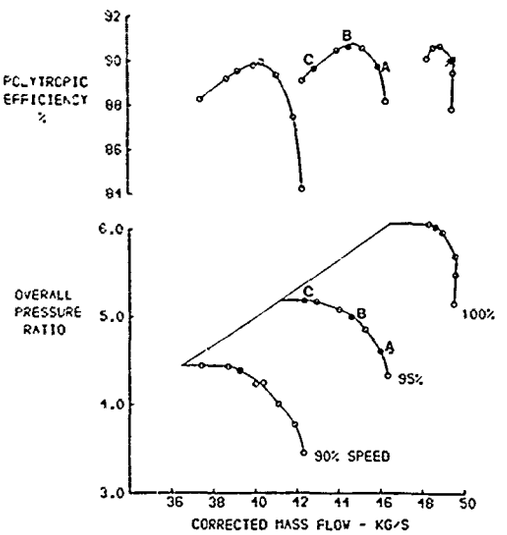

Fig. 1 The performance characteristics of C147 build 2; A, B and C denote traverse operating points.

Table 1

Compressor/probe geometry			
	Rotor 0	Rotor 1	Rotor 2
Tip speed (m/s)*	313	304	299
Blade passing frequency (Hz)*	8623	10588	11680
Mean chord (m)	0 0590	0 0485	0 0440
Mean aspect ratio	1.559	1.296	1 034
Mean pitch-chord ratio	0 551	0 550	0.552
Probe diameter / Mean pitch	0 049	0 059	0 065
X** / Mean rotor chord	0.154	0 195	0 208

* At 95% speed
** X = Mean streamwise distance from rotor trailing edge to the transducer diaphragm

Fig. 2 The pressure probe used during the traverses.

Traverse Probes

Three probes were used to take the unsteady pressure measurements. Each contained a single Kulite type XCQ-062 (344 kPa absolute) pressure transducer of 1.57 mm diameter mounted 1.65 mm below a pneumatic Pitot tube as shown in Fig 2. Two of the transducers employed a 0.07 mm thick coating of silastomer rubber to protect the pressure sensing diaphragm while the third utilised a perforated metal (Kulite 'type B') screen for protection. The relative size of the probes to the rotor rows traversed is shown in Fig 3 and detailed in Table 1 along with additional information concerning the blade rows.

Unpublished measurements, taken by Oxford University for RAE, show that the natural resonant frequency of the 'coated' transducer diaphragm was of the order of 500 kHz. The frequency response characteristics ensured a 'flat' amplitude response with negligible phase angle lag over a 100 kHz bandwidth. Frequency response of the 'screened' transducer is determined by the natural resonant frequency of the screen geometry coupled to that of the cavity between the screen and the transducer diaphragm Measurements made by Oxford University show that this is 50-60 kHz Measurements taken behind rotor 0 in C147, with both types of transducer, indicate that both measurements were generally in good qualitative and quantitative agreement but that some attenuation of peak unsteadiness levels occurred with the screened transducer.

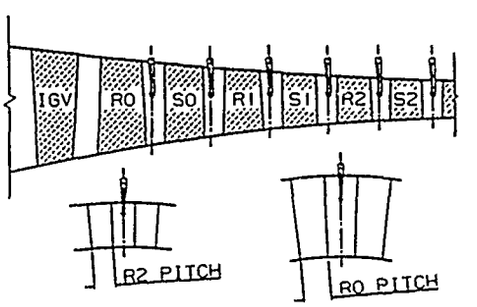

Fig. 3 The size of the traverse probe relative to the compressor.

The sensitivity of a screened transducer probe to yaw angle was measured in an open jet wind tunnel at a Mach number of 0.7. Results showed that transducer output varied by less than 1% over ± 10° range. Prior to each rotor exit traverse in C147, the probe was yawed to ensure that its axis was aligned with the mean flow at 50% span. Limited checks carried out at other radii indicated that deviation from the mean mid-span flow angle was less than ± 10 degrees.

Transducer Temperature Compensation

The strain gauge elements, that sense transducer diaphragm deflection, are prone to changes in resistance with temperature because of their high thermal coefficient of resistance. Consequently transducer pressure sensitivity and null-pressure reading (or zero-offset) change with temperature. Hence large pressure measurement errors arise if the sensitivity and zero-offset, used to convert the transducer output voltage to pressure, are not those associated with the temperature experienced by the transducer diaphragm. At RAE Bedford, Welsh and Pyne (1980) showed that if the transducer is excited with a constant voltage, changes in strain gauge bridge resistance induce a change in current drawn by the bridge which can in turn be sensed as a change in voltage across a 'sense' resistor placed in series with the transducer polarising voltage. A prototype system using this approach was produced which coupled commercially available signal conditioning amplifiers to a 'sense' resistance monitoring module (Fig 4). Setting-up of the system required the transducer to be immersed in a chamber where both pressure and temperature could be varied. Hence, the transducer pressure sensitivity and zero-offset were determined from the transducer output (Vo) for a range of constant temperatures. Similarly the 'sense' voltage (Vs), which is independent of pressure, was monitored. Subsequently, the variations of Vo and Vs with temperature were coded into a data processing program. Hence, during the compressor measurements, Vs was used to determine transducer diaphragm temperature which in turn was used to derive the associated pressure sensitivity and zero-offset in order to convert Vo to the correct absolute pressure level.

Ideally the calibrated performance of a transducer should not change significantly with time. However measurements taken at RAE have recorded transducer 'calibration drift' corresponding to up to 1% of tranducer full scale deflection over several weeks. This calibration drift was quantified by calibrating the transducers several times during the test series. Further information concerning the compensation system and how it is implemented together with details of the transducer characteristics are reported by Cherrett (1990).

The transducer temperature compensation and signal conditioning units were installed adjacent to the compressor rig. The signals were amplified and transmitted to the data acquisition system in the facility control room.

Data Acquisition and Processing

The unsteady pressure signals were recorded on a CEL Datalab Multitrap data acquisition system. This consists of three main components: a waveform recorder, a 20 Mbyte Winchester disc and a host Hewlett Packard HP310 micro-computer. The RAE system is capable of sampling 17 channels simultaneously at up to 1 MHz with better than 10-bit accuracy. The analogue-to-digital storage modules have a capacity of 256K samples per channel and can be partitioned into segments which allow the capture of data sampled to a once-per-revolution trigger signal. This trigger pulse was generated using an inductive probe to monitor the passing of a ferrite tipped rotor 2 blade. On receipt of the first pulse, the recorder is switched on to record the passing of a predetermined number of blade passages and the data stored in the first memory segment. After a complete rotor revolution, the second trigger pulse initiates sampling of the same blade passages, and the data stored in the second memory segment. This continues until the memory is full. The data are then downloaded to the micro-computer where they are processed on-line, to yield the periodic and random fluctuations within the pressure signals and subsequently stored on disc. The equations used to derive these parameters are given in the Appendix. The signals were captured at a 1 MHz sample rate which allowed 115 samples per rotor 0 passage and 85 per rotor 2 passage. Typically records of 512μS duration were captured on receipt of each trigger pulse and the data base built up over 128 consecutive rotor revolutions. Table 2 details the number of blade passages covered by each 512μS data set and also indicates the radial extent of the measurements and the type of probe used (ie, 'B-screen' or silastomer rubber coated). Continuous instantaneous data records were also captured typically recording 2 complete rotor revolutions. These were subsequently subjected to spectral analysis.

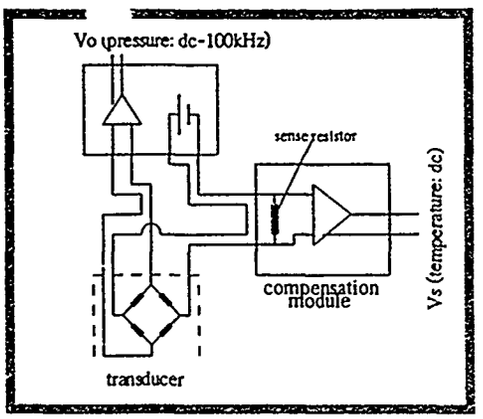

Fig. 4 The transducer temperature error compensation system.

Table 2

Radial and circumferential extent of the rotor exit measurements

	Rotor 0	Rotor 1	Rotor 2
No of radial measurements.	16	16	12
Measurement nearest tip (% span).	97.1	98 6	91 8
Measurement nearest hub (% span).	2.7	6.9	7.7
No. of rotor blade passages recorded.	4.3	5.4	6 0
Transducer type used	'B-screen' & silastomer coated.	Silastomer coated.	'B-screen'

TEST RESULTS

Time Averaged Total Pressure Measurements

Fig 5 illustrates the spanwise variation of time averaged total pressure measured at exit from rotor 0 while operating at peak efficiency (point B). The data are expressed as a ratio of total pressure at compressor inlet. The results contain an indication of the extent of absolute pressure uncertainty due to 'calibration drift'. This corresponds to ± 2.7% of reading behind rotor 0, ± 0.8% behind rotor 1 and ± 1.1% behind rotor 2. These figures could have been reduced by carrying out more frequent calibrations. Fig 5a and 5c show that agreement between the transducer and adjacent Pitot measurements is within 2% behind rotors 0 and 1 respectively.

In addition to this encouraging quantitative agreement, the profiles are in excellent qualitative agreement. Because the adjacent Pitot is far less sensitive to yaw angle than the transducer, it may be concluded that no significant errors were incurred in the transducer measurements through traversing at a fixed yaw angle. Unfortunately no adjacent Pitot measurements were taken at peak efficiency operation behind rotor 2. However, those taken behind rotor 2 at near choke flow and near surge were found to agree with the transducer results to within 0.5%. Pneumatic measurements were also taken using Pitot tubes mounted on the stator blades. At peak efficiency operation only those at rotor 1 and rotor 2 exit were available. Figs 5b and 5c show that agreement with the transducer data is less satisfactory than the adjacent Pitot measurements, especially away from mid-span. However, it should be noted that these two measurements were not made in the same meridional plane and hence not in the same position relative to upstream stator wakes and other bladerow interference effects. While overall agreement between the transducer and pneumatic measurements is encouraging and instils confidence in the temperature error compensation system, it must be borne in mind that the pneumatic measurements are subject to uncertainty due to possible averaging effects in the transmission lines. These are difficult to quantify accurately. Hence the transducer measurements are further compared with predictions arising from throughflow analysis. This shows that agreement to within 1.75% is found behind rotor 0 and rotor 2 at mid-span. Agreement behind rotor 1 is within 2.75%.

It is interesting to note the development of the extent of the annulus wall flows. At the tip, significant total pressure deficit (associated with the endwall boundary layer and over-tip leakage flow) is noted beyond 95% span in the rotor 0 measurements. In the rotor 1 and 2 measurements dynamic head decrease begins at 90% and 82% span respectively. At the hub however, rather than the expected fall in total pressure within the hub-annulus boundary layer, it is observed to increase. This is thought to be a consequence of kinetic energy imparted to the fluid by the rotating endwall.

Rotor Exit Unsteadiness

Fig 6 shows the instantaneous total pressure fluctuations measured behind rotor 0 at peak efficiency operation (point B). Data at three radii are illustrated, ie, near the hub (38% span), at mid-span (51% span), and near the tip (86% span). Included in the same figure are measurements reproduced from Ng & Epstein (1985) taken at the same spanwise stations behind a NASA Lewis transonic fan. The NASA rotor is fully transonic with inlet relative Mach numbers varying between 0.75 and 1.35 from hub-to-tip while C147 rotor 0 inlet relative Mach number varies from 0.79 at the hub to 0.94 at the tip at 95% speed. Despite the difference in shock system strength between the two rotors, the instantaneous pressure measurements are remarkably similar in qualitative appearance. That is, at the hub, the blade wakes are clearly visible as strong absolute total pressure deficits while their strength diminishes with

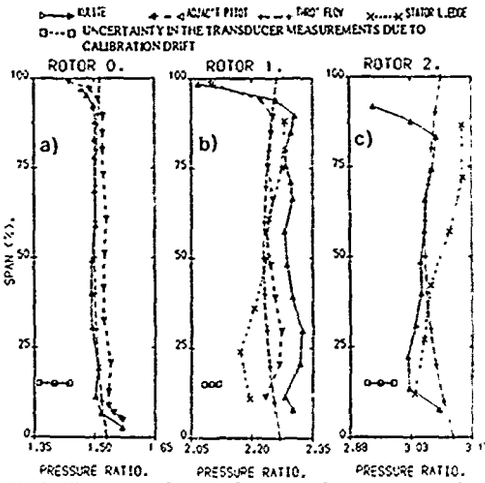

Fig. 5 Time-averaged transducer total pressure ratio measurments taken at peak efficiency operation.

increasing span. Most striking are the pressure oscillations in the inviscid core flow. These are noted in both rotor flows and are charactersed by a frequency three or four times that of blade passing. Spectral analysis of the C147 rotor 0 data confirm that the oscillations are primarily second and third harmonics of rotor 0 blade passing. No frequencies that could be attributed to downstream rotors are evident. In the NASA rotor they were seen to increase in amplitude by a factor of two in moving from hub to tip. In the C147 case, although they appear more significant because of the decrease in wake total pressure deficit, the intra-passage oscillations are of similar amplitude over much of the blade span. Quantitatively the strength of the intra-passage oscillations represents 6% of the NASA rotor total pressure ratio at the tip and 4% at mid-span. The C147 intra-passage oscillations represent 4-5% of rotor total pressure ratio.

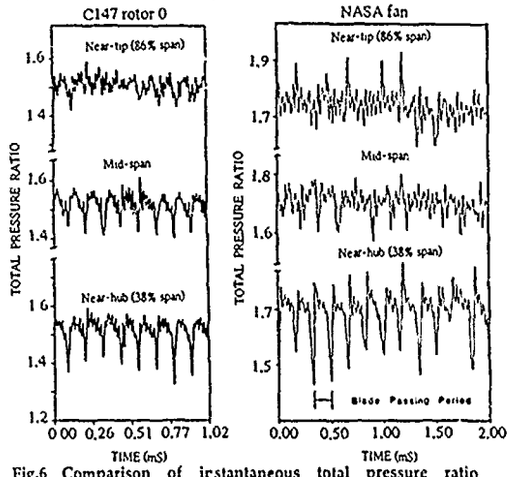

Fig.6 Comparison of instantaneous total pressure ratio measurements taken behind C147 rotor 0 and a NASA Lewis transonic fan.

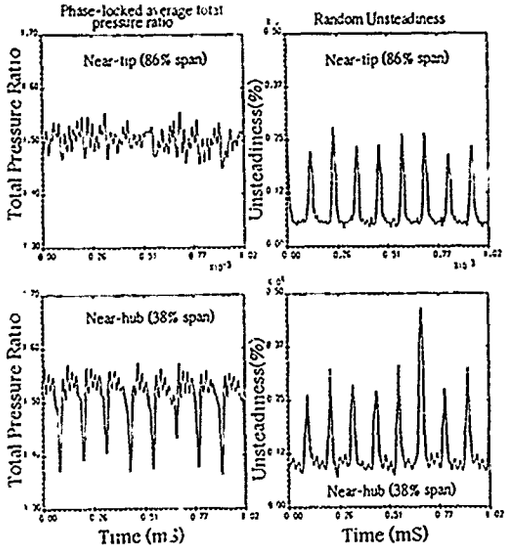

Fig. 7 Phase-locked average total pressure ratio and random unsteadiness measurements taken behind C147 rotor 0 at peak efficiency operation.

Fig 7 presents the data derived from processing the 128 segments of instantaneous data sampled in response to the once-per-revolution trigger pulse Measurements at 38% and 86% span taken behind C147 rotor 0 during peak efficiency operation (point B) are shown. Both periodic (or phase-locked average) pressure variations and the random unsteady pressure fluctuations are depicted It is evident from comparison of these data with the C147 measurements in Fig 6 that the intra-passage pressure oscillations are largely stable in the rotor relative frame and characterised by stable differences from one passage-to-another. These observations are in variance with the measurements of Ng (1985) where the ensemble averaging process, to derive the phase-locked average total pressure field, obliterated much of the intra-passage oscillation amplitude for the NASA rotor. Hence Ng & Epstein (1985) and Gertz (1986), in discussion of similar findings associated with two other transonic fan rotors, concluded that the oscillations were unstable in the rotor relative frame Ng & Epstein postulated that the intra-passage total pressure fluctuations arose from oscillation of the rotor shock system. Further, Epstein et al (1986) suggested that the shock oscillation was driven by vortex shedding in the blade wakes The arguments presented for shock oscillation being the primary mechanism are certainly convincing and it is difficult to imagine what other unstable system would give rise to similar results However, as the Mach numbers associated with C147 rotor 0 are so much lower than for the transonic fans tested it is difficult to reconcile the quantitative similarity of the measurements However, as the C147 intra-passage oscillations are stable in the rotor relative frame, while they were not in the other transonic rotors, it is conceivable that some degree of aerodynamic coupling is present in the C147 field which was not present in the other compressors

The effects of compressor operating point and bladerow interaction

In the previous discussion, the phase-locked average (ie, periodic) and random unsteady pressure fluctuations were presented as single pressure-time traces. However, while this form of presentation lends itself to detailed consideration of the measurements it does not provide a convenient way of assessing the overall flowfield. Hence, the data have been further processed to provide a pictorial representation of the flowfield variation with span. The random unsteadiness field provides a convenient tool with which to assess the salient features and spatial extent of the viscous flowfield and as such will be considered first. The phase-locked average field will then be discussed. It should be noted that the phase-locked average pressure field must be interpreted carefully because the pressure variations depicted represent absolute total pressure variations while it is intuitive to think in terms of the rotor relative field during their interpretation. Consequently these data are somewhat limited in the information they can provide concerning the aerodynamic performance of the associated rotor. This underlines the need to employ probes capable of measuring unsteady flow angle variation, with which it would be possible to transpose the measurements to the rotor relative field. To this end, RAE have procured two dynamic yawmeters of the type described by Cook (1989). These will permit measurement of unsteady tangential flow angle. In addition RAE are engaged in collaborative programmes to fund the development of probes capable of resolving 3D unsteady flow angle variation Such probes will play an important role in future work at RAE

The effects of compressor operating point on the viscous field, manifest in the random unsteadiness data, are shown in Figs 8 and 9 where measurements taken at near choke flow (A) and near surge (C) behind all three rotors are presented respectively. Data taken at peak efficiency (B) have been excluded for brevity although it should be pointed out that these measurements bear close qualitative agreement to those at near choke flow. The random unsteady fluctuations in Figs 8 and 9 are quantified as a percentage of local rotor exit total pressure

It can be seen from Fig 8 that the random unsteady flowfield recorded behind all three rotors at near choke flow exhibit strong similarities The flow is repeatable from one passage to another and is characterised by three regions. (1) an inviscid intra-blade core flow, (2) 2D-type blade wakes away from the endwalls, (3) regions of vortical activity in the hub endwall-wake area and towards the tip casing. The vortical activity toward the hub is thought to indicate separation of the suction surface/endwall boundary layer due to low momentum fluid in the endwall boundary layer being swept into the endwall-corner under the action of the cross passage pressure gradient. The extent of these features bears close similarity to high loss regions measured behind low-speed rotors by Dring et al (1982), Lakshminarayana et al (1985) and by Dong et al (1987). The measurements shown in Fig 8 indicate that these features are offset slightly to the pressure surface side of the 2D wake flow; this is probably a consequence of different amounts of underturning within the endwall-corner separation relative to that in the 2D wake and the fact that the measurements were taken some way downstream of the rotor trailing edge (see Table 1). It is interesting to note that the spatial extent of these features increases within successive rotors. At the blade tip, the regions of high random unsteadiness appear to be positioned towards the pressure surface side of the nearest blade wakes However, the blade tip clearance levels measured during the test series indicated tip-gaps of the order of 1% span which is not consistent with the existence of large scraping vortices (Inoue & Kuromaru (1989)). Rather, it is thought that the observed vortical flow is due to tip clearance flow and that the observed spatial position, relative to the 2D-type wake, is a consequence of cross passage migration and the fact that the measurements were taken downstream of the rotor trailing edge. Indeed, this is borne out by measurements (not presented in this paper) of the unsteady

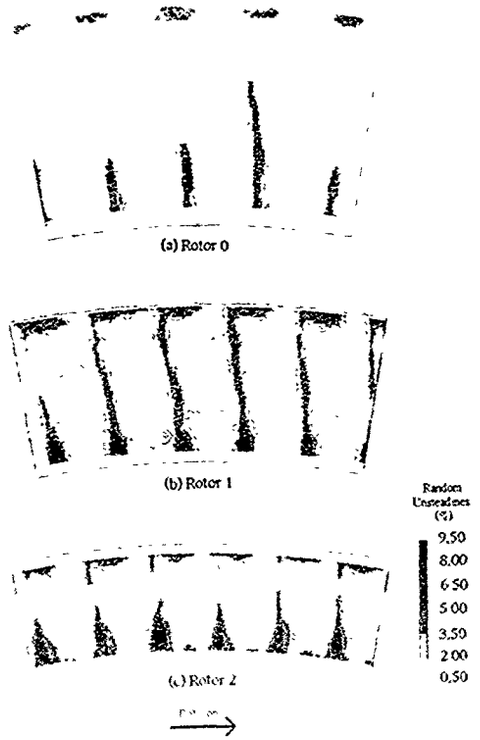

Fig. 8 Random unsteadiness measured at near choke flow (ie, Condition A).

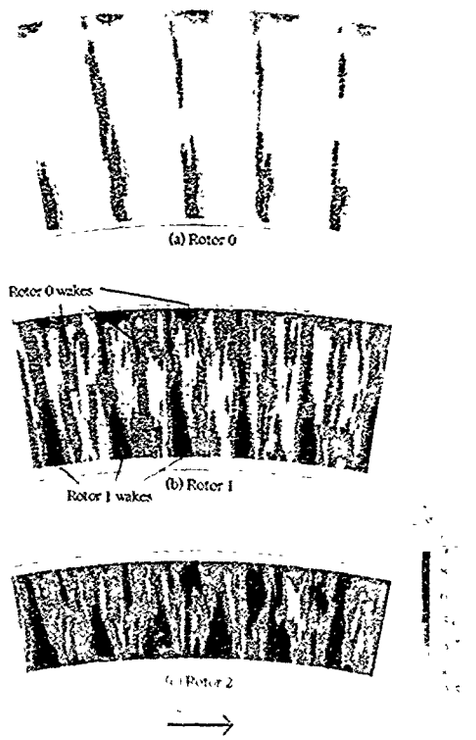

Fig 9 Random unsteadiness measured at near surge flow (ie, Condition C).

static pressure field over C147 rotor 0 in which it was possible to trace cross passage migration of the tip clearance flow consistent with the above observations

Attention is now turned to the near surge data (C) shown in Fig 9. While increasing compressor pressure ratio from point A to B (not illustrated in this paper) was accompanied by very little change in the qualitative and quantitative extent of the random unsteady flowfields, the change in moving from point B to C is marked. Behind rotor 0, the previously unadulterated core flow (Fig 8a and 9a), is now characterised by markedly higher levels of unsteadiness particularly between 50% span and the tip Also, the rotor 0 blade wakes are seen to thicken (to 20-25% pitch compared with 10-15% at lower pressure ratios) In addition, the wake flow is not so readily characterised by the distinct coexistence of hub-endwall corner separation and 2D-type wakes, the former being notably less in evidence. Similar behaviour has been observed in measurements taken behind a low-speed compressor rotor operating at different pressure ratios by Dring et al (1982)

The corresponding near surge data for rotors 1 and 2 become progressively more complex due to the effect of upstream blade wakes. In the rotor 1 measurements (Fig 9b) it is possible to attribute the most influential upstream wakes to rotor 0 through consideration of their pitch and orientation, although chopped stator 0 wakes are also visible That the major upstream blade row influence, other than that of rotor 1, originates from rotor 0 was also confirmed by spectral analysis of the instantaneous data This indicated a strong fundemental rotor 0 blade passing frequency component. Because of the different number of rotor 0 and rotor 1 blades (79 and 97 respectively) some of the rotor 0 wakes pass unimpeded through the rotor 1 passages whereas others impinge upon, or pass close to, the rotor 1 blades themselves. Where close proximity occurs the rotor 1 unsteadiness is augmented, particularly in the endwall corner separation. As this phenomenon is related to the number of blades in each row, a cyclic "waxing and waning" of the rotor 1 unsteadiness is set up about the annulus which in this case is locked to the rotating reference frame. Detailed examination of the data reveals maximum endwall-corner separation unsteadiness levels are attained every 6 to 7 rotor 1 blades. This is commensurate with rotor-rotor interaction between stages 0 and 1

Examination of the rotor 2 field (Fig 9c) reveals that a number of upstream blade wakes are evident. Spectral analysis of instantaneous data reveals that the most influential upstream influences are rotor 0 and rotor 1. However, whereas it was quite possible to arrive at the same conclusion through subjective examination of the rotor 1 field, this is not possible for rotor 2 due to the complexity of the data The progressive increase in complexity of the rotor exit field is commensurate with the attention being shifted to more embedded rotor flows. Fig 10 presents the circumferentially

TM p 1198

averaged variation of random unsteadiness with span for the rotor exit flows at the three operating points. These data reinforce the trends already noted in the discussion of Figs 8 and 9. That is, (1) the level of random unsteadiness rises within successive rotor flows at the same operating point, (2) increasing compressor pressure ratio (ie rotor loading) increases the intensity of the random unsteady field However, the increase in intensity of the random unsteady field becomes more marked as compressor surge is approached.

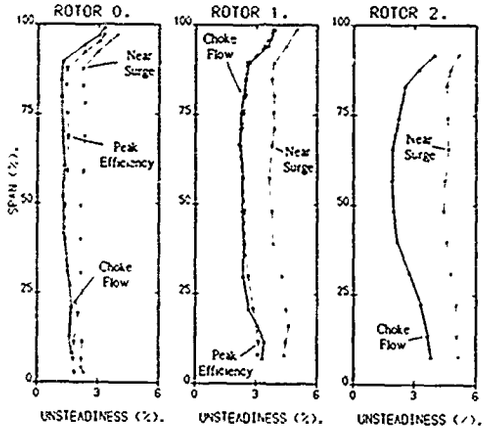

Fig. 10 Time-averaged random unsteadiness measured behind rotors 0, 1 and 2.

Attention is now turned to the ac-coupled phase-locked average (periodic) pressure field Qualitatively the appearance of the data did not change dramatically with operating condition as observed for the random unsteadiness data Hence, only the near surge (point C) data are presented in Fig 11 where they are quantified as a percentage of local time-averaged total pressure at rotor exit. However, while the data at different operating points were qualitatively similar, their quantitative extent (particularly behind the embedded rotors) did change.

From Fig 11a it can be seen that the excess total pressure oscillations, noted previously in Figs 6 and 7, dominate the rotor 0 intra-passage flowfield Further, these features are aligned radially to form coherent structures extending over much of the blade span However, they are particularly apparent in the lower half of the annulus The quantitative extent of the range of maximum to minimum pressures encountered in the flowfield is similar at the three operating conditions That is, for the rotor 0 measurements illustrated in Fig 11a, they range between +5.7% and -11.0% while figures of +6.5% to -14.1% and +6.8% to -10.9% were recorded at near maximum flow and peak efficiency operation The rotor 1 and 2 periodic flowfields are significantly different from the rotor 0 data in their appearance. While the rotor 0 field is quantitatively repeatable from one passage to another this is not so behind rotors 1 and 2 That is, although radially aligned intra-passage total pressure excess regions are seen behind rotors 1 and 2 the flow is dominated by localised pressure excess regions These are found towards the tip in the rotor 1 field and at both hub and tip behind rotor 2. The strength of these features is not repeatable from one passage to another Rather, their intensity "wax and wane" over a wavelength consistent with the rotor-rotor interaction observed in the random unsteadiness data described earlier The peak pressures attained in these regions equate to 9.9% and 10.6% of the local time-averaged total pressures encountered behind rotor 1 and rotor 2 respectively. These peak pressure levels were noted to increase significantly with increasing compressor pressure ratio. That is, the peak pressure excess levels in the rotor 1 field increase by 18% in moving from choke flow to near surge. Similarly a 24% increase accompanies the movement from choke flow to near surge operation behind rotor 2. Of course in the absence of unsteady flow angle measurements it is difficult to ascertain to what extent these absolute total pressure excess regions are manifestations of relative flow angle or relative total pressure fluctuations However, it is interesting to note that in the rotor 1 measurements the strongest total pressure excess regions in the phase-locked average field were found in the same blade passages that contained the most vigorous hub-corner vortical activity as measured in the random unsteadiness field.

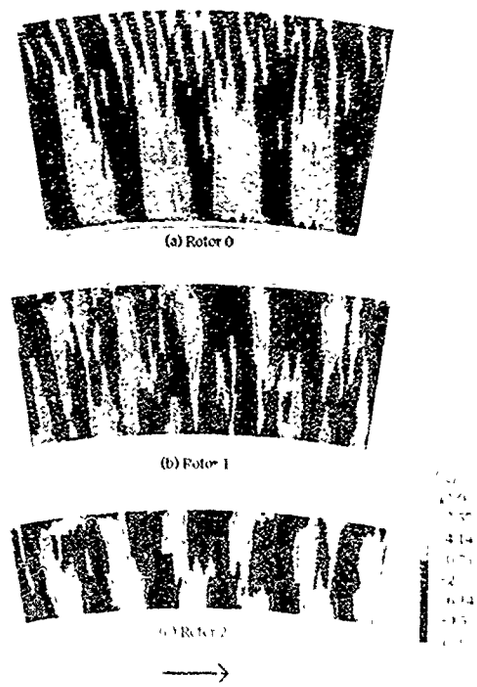

Fig. 11 AC-coupled phase-locked average total pressure expressed as a percentage of local time-averaged total pressure. All of the measurements were taken at near surge operation.

CONCLUSIONS

A high frequency response total pressure probe has been traversed behind the first three rotors of a high-speed five stage core compressor (C147) Measurements were taken at maximum flow, peak efficiency, and near surge operation at 95% speed Major conclusions resulting from the work are outlined below.

1. A reliable, and easily implemented approach to correcting semi-conductor transducer temperature errors has been applied successfully Comparisons between transducer

time-averaged pressure measurements, and pneumatic pressure measurements show agreement within 2-3% This gives confidence in the temperature compensation system but more work is required to improve accuracy.

2 In the case of the first stage rotor, strong total pressure oscillations of 3-4 times blade passing frequency were observed in the inviscid intra-passage flow. These appeared stationary in the rotor relative frame which is at variance with measurements taken in single-stage transonic fans.

3 The random unsteady pressure flowfield measured at exit from the C147 rotors showed the nature and extent of the inviscid core flow as well as the viscous wake, hub-endwall separation, and over-tip leakage flow regions. The wake and hub-endwall separation regions increased in size and level of random pressure unsteadiness as compressor pressure ratio was increased

4 At a given compressor operating point, the tip-leakage and hub-endwall separation regions were found to grow in size, for successive downstream rotors and hence occupy a more significant portion of the rotor exit flow

5 In the embedded stage rotors, strong rotor-rotor interaction effects were noted These induced waxing and waning of the size and intensity of the zones of peak unsteadiness at the hub and excess phase locked total pressure at the tip

6 An encouraging start has been made in a continuing programme of research into unsteady compressor flows at RAE Pyestock However, single sensor probe measurements provide limited information 2D and 3D multisensor probes will be used in future compressor research at RAE

REFERENCES

Calvert, W J, Ginder, R B, McKenzie, I R I, Way, D J 1989, "Performance of Highly Loaded HP Compressor," ASME Paper No 89-GT-24

Cherrett, M A, 1990, "Temperature Error Compensation Applied to Pressure Measurements Taken with Miniature Semiconductor Pressure Transducers in a High-Speed Research Compressor," Proceedings, 10th Symposium on Measuring Techniques for Transonic and Supersonic Flows in Cascades and Turbomachines, Von Karman Inst, Brussels, Belgium

Cook, S C, 1989, 'Development of a High Response Aerodynamic Wedge Probe and Use on a High-Speed Research Compressor" Proceedings of the Ninth International Symposium on Air Breathing Engines Vol 1, pp 1113-1125

Dong, Y, Gallimore, S J, and Hodson, H P, 1987, "Three-Dimensional Flows and Loss Reduction in Axial Compressors," ASME Journal of Engineering for Power, Vol 109, pp 354-361

Dring, R P, Joslyn, H D, and Hardin, L W, 1982, "An Investigation of Axial Compressor Aerodynamics," ASME Journal of Engineering for Power, Vol 104, pp 84-95

Epstein, A H, Gertz, J B, Owen, P P, and Giles, M B, 1986, "Vortex Shedding in Compressor Blade Wakes," Proceedings, Transonic and Supersonic Phenomena in Turbomachines, AGARD-CP-401, pp 5 1-5 13

Gertz, J B, 1986, 'Unsteady Design-Point Flow Phenomena in Transonic Compressors," MIT Report GTL No 188

Ginder, R B, 1991, 'Design and Performance of Advanced Blading for a Highly-Loaded HP Compressor,' ASME Paper IGTI 91

Inoue, M, and Kuromaru, M, 1989, "Structure of Tip Clearance Flow in an Isolated Axial Compressor Rotor," ASME Journal of Engineering for Power, Vol 111, pp 250-256

Lakshminarayana, B, Sitaram, N, and Zhang J, 1985, "End-Wall and Profile Losses in a Low-Speed Axial Flow Compressor Rotor,"
ASME 85-GT-174

Lakshmunarayana, B, and Govindan, T.R., 1981, "Effects of Rotation and Blade Incidence on the Properties of the Turbomachinery Rotor Wake," AIAA Paper No AIAA-81-0054

Ravindranath, A, and Lakshminarayana, B, 1980, "Mean Velocity and Decay Characteristics of the Near and Far-Wake of a Compressor Rotor Blade of Moderate Loading," ASME Journal of Engineering for Power, Vol 102, pp. 535-548.

Ng, W F, and Epstein, A H, 1985, "Unsteady Losses in Transonic Compressors," ASME Journal of Engineering for Gas Turbines and Power, Vol 107, pp 345-353.

Wagner, J H., Okiishi, T H, and Holbrook, G J., 1978, "Periodically Unsteady Flow in an Imbedded Stage of a Multistage Axial-Flow Turbomachine," ASME 78-GT-6.

Welsh, B, and Pyne, C.R, 1980, "A Method to Improve the Temperature Stability of Semiconductor Strain Gauge Transducers", Journal of Physics E Science Instrumentation, Vol 13, pp 816-818.

Weyer, H B, and Hungenbert, H G., 1975, "Analysis of Unsteady Flow in a Transonic Compressor by Means of High-Response Pressure Measuring Techniques," Proceedings, Unsteady Phenomena in Turbomachinery, AGARD-CP-177.

Zierke, W.C, and Okiishi, T H, 1982, "Measurement and Analysis of Total-Pressure Unsteadiness Data from an Axial-Flow Compressor Stage," ASME Journal of Engineering for Power, Vol. 104, pp 479-488

APPENDIX PROCESSING OF THE PHASE-LOCKED DATA

The multiple instantaneous records captured in resonse to the once-per-revolution trigger pulse were processed in the following manner to determine the periodic (phase-locked average) and random fluctuations within the pressure transducer signals.

a The phase-locked average V(t) is defined as the sum of the individual instantaneous data records meaned over the number of rotor revolutions (or instantaneous data records) recorded, ie

$$V(t) = \frac{1}{N} \sum_{k=1}^{N} V_k(t)$$

where, $V_k(t)$ = instantaneous data values

N = number of rotor revolutions

b The random unsteadiness $V_r(t)$ is determined by comparing each instantaneous data trace with the phase-locked average trace, squaring the difference between the two traces, summing and meaning over N revolutions, and finally dividing by the time-averaged dc component of the phase-locked average V(t) ie,

$$V_r(t) = \frac{\sqrt{\frac{1}{N} \sum_{k=1}^{N} \left| V_k(t) - V(t) \right|^2}}{V(t)}$$

REPORT DOCUMENTATION PAGE

Overall security classification of this page

UNLIMITED

As far as possible this page should contain only unclassified information. If it is necessary to enter classified information, the box above must be marked to indicate the classification, e.g. Restricted, Confidential or Secret.

1. DRIC Reference (to be added by DRIC)	2. Originator's Reference	3. Agency Reference	4. Report Security Classification/Marking
	RAE TM P 1198		UNLIMITED

5. DRIC Code for Originator	6. Originator (Corporate Author) Name and Location
7674300E	Royal Aerospace Establishment, Pyestock, Hants, UK
5a. Sponsoring Agency's Code	6a. Sponsoring Agency (Contract Authority) Name and Location

7. Title Unsteady viscous flow in a high speed core compressor

7a. (For Translations) Title in Foreign Language

7b. (For Conference Papers) Title, Place and Date of Conference

8. Author 1. Surname, Initials	9a. Author 2	9b. Authors 3, 4	10. Date	Pages	Refs.
Cherrett, M.A.	Bryce, J.D.		December 1990	10	10

11. Contract Number	12. Period	13. Project	14. Other Reference Nos.

15. Distribution statement

(a) Controlled by –

(b) Special limitations (if any) –

If it is intended that a copy of this document shall be released overseas refer to RAE Leaflet No.3 to Supplement 6 of MOD Manual 4.

16. Descriptors (Keywords) (Descriptors marked * are selected from TEST)

Turbomachinery*. Axial flow compressors*. Unsteady flow*. Unsteady pressure measurement*. Turbulence*. Pressure sensors*. C147.

17. Abstract

A probe incorporating a miniature high-frequency response pressure transducer has been traversed behind the first three stages of a high-speed multistage compressor operating at throttle settings corresponding to near choke, peak efficiency and near surge. A novel method of compensating for transducer temperature sensitivity was employed. Consequently, time-averaged pressures derived from the transducer were found to be in good agreement with pneumatic pressure measurements. Analysis of the unsteady pressure measurements revealed both the periodic and random fluctuations in the flowfield. This provided information on rotor-rotor interaction effects and the nature of viscous blade wake and secondary flows in each stage.

F5910/1

RAE Form A143 (revised October 1980)